

A Confining Strong First-Order Electroweak Phase Transition

Germano Nardini^a, Mariano Quirós^{a,b} and Andrea Wulzer^a

^a *IFAE, Universitat Autònoma de Barcelona, 08193 Bellaterra, Barcelona (Spain)*

^b *Institució Catalana de Recerca i Estudis Avançats (ICREA)*

Abstract

In the Randall-Sundrum model where the radion is stabilized by a Goldberger-Wise (GW) potential there is a supercooled transition from a deconfined to a confined phase at temperatures orders of magnitude below the typical Standard Model critical temperature. When the Higgs is localized at the IR brane the electroweak phase transition is delayed and becomes a strong first-order one where the Universe expands by a few e-folds. This generates the possibility of having the out-of-equilibrium condition required by electroweak baryogenesis in the electroweak phase transition. We have studied numerically the region of the GW parameter space where the theory is consistent and the latter possibility is realized. We have found that in most of the parameter space the nucleation temperature is so low that sphalerons are totally inactive inside the bubbles. The condition for sphalerons to be inactive after reheating imposes an upper bound on the reheating temperature that is weaker for heavy Higgs bosons so that the out-of-equilibrium condition seems to favor heavy over light Higgses. The condition for sphalerons to be active outside the bubbles puts an upper bound on the number of e-folds at the phase transition, roughly consistent with the critical value required by low-scale inflation to solve the cosmological horizon problem.

1 Introduction

The Standard Model (SM) of electroweak interactions is being tested to high accuracy at present (e.g. Tevatron) and past (e.g. LEP) colliders and the physics it describes will be probed at the future LHC at CERN. In spite of its impressive experimental successes the SM has a number of theoretical and experimental drawbacks that make it difficult to be considered as a fundamental theory. In particular, from the experimental side the SM does not have a good candidate for the Dark Matter of the Universe while on the theoretical side it exhibits a number of problems as e.g. the unnatural fine-tuning it requires to accomodate the weak scale along with heavier ones, as the Planck scale. In order to solve some of these problems several extensions of the Standard Model have been proposed so far. The most popular of them, the minimal supersymmetric SM extension (MSSM) which solves the big hierarchy problem and provides interesting candidates to Dark Matter, shares some of the other SM problems. A completely different solution to the hierarchy problem was proposed in Ref. [1] where the Higgs field is localized in a four-dimensional (4D) brane inside a five-dimensional (5D) space with a warped fifth dimension: the warping red-shifts large (Planck-sized) scales to TeV ones, thus solving the big hierarchy problem. More recently, warped models with matter in the bulk have been widely discussed with the aim of finding a solution to the little hierarchy problem as well. An incomplete list includes Higgsless theories [2, 3], in which the electroweak symmetry is broken by boundary conditions and no Higgs scalar is needed, and models of Gauge-Higgs Unification in warped space [4]-[7]. The latter scenario is also interpreted, via AdS/CFT, as a calculable version of Composite-Higgs and appears particularly promising.

An interesting feature of the SM is that it contains baryon number violation by non-perturbative effects (sphalerons at finite temperature) that have the capability to generate the baryon asymmetry of the Universe at the electroweak (EW) phase transition via the so-called EW baryogenesis (EWBG) mechanism [8]-[11]. Unfortunately one of the requirements of EWBG, a strong first-order phase transition, was soon proved not to be fulfilled in the Standard Model, thus preventing this appealing possibility. While the possibility of having a strong enough first-order phase transition is marginal in the MSSM [12] we will prove in this paper that the Randall-Sundrum (RS) theory provides in a natural way a supercooled first-order electroweak phase transition that can accomodate the mechanism of EWBG provided an extra source of CP -violation is generated. The main point of the mechanism is that the radion delays the electroweak phase transition till temperatures much lower than the electroweak one where the order parameter of the Higgs effective potential $\phi(T)/T$ is large. We summarize in the rest of this section the essential points of this mechanism.

At finite temperature [13] there are two stationary solutions of the 5D gravity partition function. One is the usual RS geometry with two branes located on the UV and the IR points respectively. The other one corresponds to AdS-Schwarzschild (AdS-S) geometry where the IR brane is replaced by a black-hole horizon. Using the AdS-CFT correspon-

dence both phases correspond in 4D respectively to confined and deconfined strongly interacting gauge theory. Because conformal invariance is only spontaneously broken in the confined phase the free thermal energy of the AdS-S phase is lower than that of the RS phase and thus the latter is metastable. However after explicitly breaking conformal invariance of the RS phase, e.g. by the introduction of a 5D field which creates a potential for the radion stabilizing the distance between the UV and IR branes as in the Goldberger-Wise (GW) model [14], the free energy of the confined and deconfined phases becomes equal at a given critical temperature and for lower temperatures the phase transition from the AdS-S to the RS phase can proceed. We have studied numerically the process of bubble formation (of the IR brane out of the black-hole horizon) and found that ¹, though the critical temperature lies in the sub-TeV region the actual nucleation temperature is orders of magnitude below, essentially due to the flatness of the radion stabilizing potential. Thus the radion phase transition is a supercooled one and it corresponds to a strong first-order phase transition.

On the other hand the Higgs is localized on the IR brane: it can be either exactly localized or exponentially localized, in both cases it corresponds to a composite object from the holographic point of view ². In the AdS-S phase, then, the Higgs is deconfined and so from an effective theory point of view it can be described as being in the symmetric phase $\phi = 0$. In the RS phase the Higgs field appears [confines] and so the possibility of having $\phi \neq 0$ opens up. The radion supercooling prevents then the Higgs phase transition to proceed at typical electroweak temperatures. When the barrier between the deconfined and the confined phases is sufficiently low to be overcome by a quantum jump at low temperatures the ratio $\phi(T)/T$ can be large and the electroweak phase transition becomes a strong first-order one. In the present article, for simplicity, we restrict ourselves to the case of an exactly localized Higgs. In the conclusion we will comment on how this mechanism can be applied to other scenarios like Higgsless or gauge-Higgs unification theories.

The contents of this article are as follows. In section 2 we describe the two phases, RS and AdS-S, from the holographic point of view and the free energy of both phases is provided. In section 3 we add the Goldberger-Wise bulk field in order to stabilize the radion potential and the Higgs localized in the IR brane that provides a vacuum expectation value (VEV) to spontaneously break the electroweak symmetry. We identify the region in the parameter space where there is a stable minimum fixing the radion VEV and where the back-reaction on the RS metric is small and the theory is consistent. In section 4 the phase transition is analyzed in some detail using both numerical methods and analytical approximations. In most of the available parameter space the Euclidean action is dominated by $O(4)$ symmetric bubbles and the nucleation temperature corresponds to a few e-folds of inflation. In section 5 we apply the results of the supercooled electroweak

¹Some preliminary analyses of the phase transition can be found in Refs. [13, 15, 16].

²The rest of the SM matter fields (fermions and gauge bosons) can be either localized in the IR brane or they can be propagating in the bulk of the fifth dimension.

phase transition to the required conditions for EWBG. Sphalerons inside the bubbles are inactive in all cases because the nucleation temperature is far lower than the SM phase transition temperature. Sphalerons have to be active outside the bubbles and this leads to an upper bound on the number of e-folds of inflation, as $N_e < 26$, roughly consistent with the number of e-folds ($N_e > 30$) required to solve the cosmological horizon problem with TeV scale inflation [17]. A second condition is obtained from requiring sphalerons not to erase the generated baryon asymmetry after reheating, which implies a maximal reheating temperature. Counterintuitively the larger the Higgs mass the weaker this constraint becomes. This latter condition, for a given number of e-folds of inflation, translates on upper bounds on the IR scale (μ_{TeV}) -obtained from the minimum of the GW potential- as a function of the Higgs mass. This leads to values of μ_{TeV} in the TeV range at least for a moderate number of e-folds of inflation. Again the larger the Higgs mass the weaker this condition. Finally section 6 is devoted to our conclusion and a list of open problems.

2 Holography of the two Phases

The conjectured AdS/CFT correspondence [18, 19] relates extra-dimensional (stringy) models of gravity to $4D$ gauge theories formulated on the boundary of the extra space. One is often interested in the small string length limit in which the gravity side is well described by effective (super-)gravity and, according to the correspondence, the $4D$ theory has large 't Hooft coupling. The inverse loop expansion parameter for gravity is dual to the number N of colors, so that weakly coupled extra-dimensional models are dual to large- N strongly coupled $4D$ theories. In fact we will never be able to exit the strong ('t Hooft) coupling regime with our field-theoretical description because, unlike the more familiar QCD case, both the confining and deconfining phases are strongly coupled in the dual $4D$ theory we are discussing.

We will consider the Randall-Sundrum (RS) set-up [1], *i.e.* $5D$ gravity with negative cosmological constant and two four-dimensional boundaries which are called UV and IR branes. Holographically, this corresponds [20, 21] to a $4D$ conformal field theory (CFT) coupled to gravity in which the conformal symmetry is also spontaneously broken. The spontaneous breaking is an IR effect and its scale μ is associated to the position of the IR brane. The presence of the UV brane, on the contrary, explicitly breaks the conformal symmetry as it couples the theory to gravity. This occurs at an UV scale $k = L^{-1}$, where L is the AdS radius, which also represents an UV cut-off for the CFT. At the technical level, a more precise statement of the correspondence is as follows [19, 22]. The partition function $Z_4[M]$ of the $4D$ gauge theory formulated on the space M with metric g is computed as a constrained partition function for $5D$ gravity

$$Z_4[M] = \int \mathcal{D}G(x, z)_{\hat{G}=g(x)} e^{i S_{grav}[G]}, \quad (2.1)$$

where the subscript " $\hat{G} = g$ " means that the $5D$ metrics $G(x, z)$ one integrates over are only those which induce a given $4D$ metric g on the UV boundary. In Eq. (2.1) S_{grav} is

the standard 5D gravity action with boundaries and will be better specified below. Let us now briefly remind what Eq. (2.1) implies for the standard interpretation of the RS model. The l.h.s. is the partition function of the CFT calculated with a cut-off k , which contains not only conformal-invariant terms but also local (non-conformal) counterterms such as for instance an Einstein term for the 4D metric g [22]. In the RS set-up the metrics one integrates over have no constraints at the UV, so that the RS partition function is obtained by integrating again the r.h.s. of Eq. (2.1) on all the 4D metrics $g(x)$. On the r.h.s. this corresponds to make gravity dynamical with a 4D Planck scale set by the CFT cut-off k . However in our context gravity is not required to be made dynamical and all we need is Eq. (2.1) in its Euclidean version.

The thermal partition function of the 4D theory is indeed obtained by considering a space $M = S^1 \times T^3$ where the circle S^1 represents Euclidean time and the 3-torus T^3 ordinary three-space. The metric is Euclidean, the length of the circle is $\beta = 1/T$ (T is the temperature) and we will call V the volume of T^3 . At finite temperature, as noticed in [13], the 5D path integral in Eq. (2.1) has two stationary solutions at the classical level. The first one is the Euclidean version of the standard RS geometry with compactified time. It is

$$ds_{RS}^2 = \frac{L^2}{z^2} \left(\beta^2 d\tau^2 + V^{2/3} d\vec{\xi}^2 + dz^2 \right), \quad (2.2)$$

where the extra coordinate z is in the $[z_{UV} \equiv L, z_{IR} \equiv \mu^{-1}]$ interval, τ is a temporal variable with unit period and $\vec{\xi}$ span a square 3-torus of unitary volume. The second solution is the so-called AdS-Schwarzschild (AdS-S) space, with metric

$$ds_{AdS-S}^2 = \frac{L^2}{z^2} \left(\beta_h^2 (1 - z^4/z_h^4) d\tau^2 + V^{2/3} d\vec{\xi}^2 + \frac{dz^2}{1 - z^4/z_h^4} \right). \quad (2.3)$$

Also in this case we chose the extra coordinate $z \in [L, z_h]$ so that the UV brane is located at $z_{UV} = L$, but the end of the space now is not the IR brane, but the black-hole horizon z_h where the space (2.3) has, in general, a conical singularity. However, by choosing

$$z_h = \frac{1}{\pi} \beta_h, \quad (2.4)$$

we can put the deficit angle to zero and, under this condition, the space is completely regular and it is a true solution to the Einstein equations. The time periodicity β_h in Eq. (2.3) is determined by Eq. (2.1) which states that at the UV the length of the time circle must be equal to $\beta = T^{-1}$. It is

$$\beta_h^2 = \frac{\beta^2}{2} \left[1 + \sqrt{1 + 4\pi^4 (LT)^4} \right]. \quad (2.5)$$

The physical meaning of the two solutions is quite simple [13]. At finite temperature, one has two classical minima of the 5D action, and two disconnected semiclassical (loop) expansions could be carried out around each of them, leading of course to completely

different physical results. From the $4D$ dual point of view, the RS and AdS-S minima correspond to two different phases, which we identify, respectively, with the confining and deconfining phases of the gauge theory. It follows from Eq. (2.1) that the free-energies in the two phases are proportional to the (effective) actions of the two gravity solutions. Depending on the temperature, and neglecting for the moment the dynamics of the phase transition in an expanding Universe, the physical minimum is the one with lowest $5D$ action or (equivalently) $4D$ free-energy.

At the classical level one computes the free-energies by plugging the solutions (2.2) and (2.3) into the action. The latter reads

$$S_{grav}^E = -4M^3 \left[\int_{\mathcal{M}} (R + 12k^2) + \int_{\partial\mathcal{M}_{UV}} 2K_{UV} + \int_{\partial\mathcal{M}_{IR}} (2K_{IR} + 6k) \right], \quad (2.6)$$

where R is the $5D$ curvature scalar, $M \sim M_P$ the $5D$ Planck mass and $K_{UV(IR)}$ the extrinsic curvatures of the two boundaries $\partial\mathcal{M}_{UV(IR)}$. Following the conventions of [23], in Gaussian normal coordinates

$$K = \gamma^{ab} K_{ab} = \frac{1}{2} \gamma^{ab} \partial_\eta \gamma_{ab}, \quad (2.7)$$

where η is the coordinate normal to the boundary and γ the induced metric. The equations of motion associated to the action (2.6) are the $5D$ Einstein equations in the bulk plus the Israel junction condition

$$K_{ab}^{IR} = -k\gamma_{ab}^{IR}, \quad (2.8)$$

at the IR brane only. One has no junction condition at the UV because the UV metric is fixed in (2.1) and should not be varied when working out the equations of motions from the action.

While both spaces (2.2) and (2.3) solve the bulk Einstein equations only the RS geometry solves the Israel junction condition (2.8), thanks to the fine-tuned choice we did in Eq. (2.6) for the IR brane tension. On the contrary the AdS-S metric (2.3) does not solve Eq. (2.8), meaning that an IR brane cannot be put in that geometry. Thus strictly speaking both spaces (2.2) and (2.3) are not solutions of the same gravity action. In fact for the AdS-S to be a solution the IR boundary terms (last terms of Eq. (2.6)) should be dropped. One might think however that the IR brane is hidden by the black-hole horizon in the AdS-S space so that the IR terms of the action do not effectively contribute. More precisely one should think of the IR brane in RS as a remnant of a more complicated solitonic-like geometry which solves the equations of motions of a more fundamental underlying theory of gravity. The same theory should also allow for a second solution, without the brane, which would correspond to the AdS-S space.

The free-energy of the two phases is readily computed. By plugging Eq. (2.2) into Eq. (2.6) we get for the confining (RS) phase

$$F_{RS} = \frac{1}{\beta V} S_{grav}^E [RS] = -24(ML)^3 k^4, \quad (2.9)$$

which is just the usual RS bulk cosmological constant which we could have canceled by adding a suitable UV brane tension term to Eq. (2.6). For the deconfined phase we must remove the IR terms from Eq. (2.6) and plug Eq. (2.3). One gets

$$\begin{aligned} F_{AdS-S} &= \frac{1}{\beta V} S_{grav}^E [AdS - S] = -8(ML)^3 k^4 \left[\frac{\beta}{\beta_h} + 2\frac{\beta_h}{\beta} \right] \\ &= \left[-24k^4 - 4\pi^4 T^4 \left(1 + \mathcal{O} \left(\frac{\pi^4 T^4}{k^4} \right) \right) \right] (ML)^3 \end{aligned} \quad (2.10)$$

where an expansion for $\pi T \ll k$ has been performed. As a general rule of AdS/CFT, the loop expansion on the gravity side corresponds to a large number of colors (large- N) expansion in the gauge theory. The squared coupling constant for 5D gravity is $1/(ML)^3$ and naive dimensional analysis (NDA) suggests that the expansion parameter is given by the squared coupling divided by a loop factor. The precise AdS/CFT relation ³

$$\frac{1}{N^2} = \frac{(ML)^{-3}}{16\pi^2}, \quad (2.11)$$

perfectly matches this interpretation. Let us now compare the above equation with the free-energies (2.9) and (2.10). The RS phase is confining and indeed F_{RS} only contains a vacuum energy term to which all the $N^2(-1)$ confined gluons can contribute. The vacuum energy scale is fixed by the UV cut-off k of the 4D theory. The AdS-S phase, on the contrary, is deconfining and the $N^2(-1)$ massless gluons are present in the plasma everyone giving its standard $\sim T^4$ contribution. The vacuum energy, which is the same in both phases, can be always shifted to zero by adding an UV brane tension term to the action (2.6).

3 Adding the Golberger-Wise and Higgs fields

Equations (2.9) and (2.10) immediately uncover a problem: at any non-zero temperature $F_{AdS-S} < F_{RS}$ so that the RS space is metastable and no phase transition can ever occur from the AdS-S to the RS phase. This is because the conformal symmetry is only spontaneously broken in the RS phase and it is completely unbroken in the AdS-S one. Being spontaneous, the conformal breaking indeed leads to a massless Goldstone boson, the radion, which arises in 5D as a modulus of the RS geometry corresponding to the distance among the two branes [20, 21]. Having fixed the location of the UV brane, the

³The relation (2.11) can be changed by numerical factors depending on the precise theory. We will use Eq. (2.11) as a definition.

radion field controls the position μ^{-1} of the IR brane. Given that the radion is a Goldstone, it cannot have a potential and this is why it does not contribute to the vacuum energy and then to the free-energy (2.9) at leading order in the large- N expansion. Since the radion potential is flat and μ undetermined, the temperature is the only dimensionful quantity and there is no other scale the temperature can be compared with (the cut-off k is not relevant here). Stated in another way there is no scale which could fix the temperature of transition T_c . In fact starting in the AdS-S phase and lowering the temperature the system would remain in that phase forever. The same occurs for the first holographic deconfining phase transition discussed by Witten [24] in the case of unbroken conformal symmetry.

3.1 The Golberger–Wise field

Independently of the above considerations an explicit breaking of conformal symmetry is required anyhow to avoid the presence of an exactly massless scalar. The so-called Goldberger–Wise (GW) mechanism [25] permits to stabilize the distance among the branes and give a mass (and a potential) to the radion by simply adding a 5D scalar field Φ . The Euclidean action is

$$S_{GW}^E = \int_{\mathcal{M}} [G^{MN} \partial_M \Phi \partial_N \Phi + m^2 \Phi^2] + \int_{\partial \mathcal{M}_{IR}} (\mathcal{L}_{IR}(\Phi) + k^4 \delta T_1) , \quad (3.1)$$

where δT_1 amounts to a correction to the IR brane tension in Eq. (2.6). We do not need to specify the IR Lagrangian \mathcal{L}_{IR} since it only plays the role (as in [25]) of enforcing the IR boundary condition

$$\Phi(x, z_{IR}) = k^{3/2} v_1 . \quad (3.2)$$

Holographically the GW field corresponds [20, 21] to an explicit UV breaking of the conformal symmetry due to an operator \mathcal{O} of conformal dimension $d = 4 + \epsilon$ where

$$\epsilon = \sqrt{4 + m^2 L^2} - 2 \simeq \frac{m^2 L^2}{4} , \quad (3.3)$$

and we have assumed $m^2 \ll k^2$ to perform the expansion. In AdS space the squared mass of a scalar can be positive or negative and then ϵ can have both signs. To have a solution of the hierarchy problem $|\epsilon|$ must be small ($\lesssim 1/10$) and we are going to assume this in the following. Adding the GW term (3.1) to the action modifies the correspondence of Eq. (2.1) in a very simple way. On the l.h.s. one has the partition function of a different 4D theory which gets modified by the introduction of the term

$$\frac{\lambda}{k^{\epsilon+3/2}} \widehat{\Phi}(x) \mathcal{O} , \quad (3.4)$$

to the 4D Lagrangian. In the above equation λ is a dimensionless coupling, k is the UV cut-off and $\widehat{\Phi}(x)$ a non-dynamical 4D source field. On the r.h.s. of Eq. (2.1) we now have

the new $5D$ field Φ to integrate over. As for the metric one has to consider a constrained path integral. The value of Φ on the UV brane is

$$\Phi(x, z_{UV}) = \hat{\Phi} \equiv k^{3/2} v_0, \quad (3.5)$$

where we fixed the source $\hat{\Phi}$ to a constant value and then converted the operator (3.4) into a deformation of the CFT. One could also have made $\hat{\Phi}$ dynamical, and added a Lagrangian for Φ at the UV as in [25]. The role of those terms, as for \mathcal{L}_{IR} , would simply have been to enforce the boundary condition (3.5) and hence, in practice, to convert $\hat{\Phi}(x)$ back into a non-dynamical field. The two approaches are then completely equivalent.

To find the background configuration in the presence of the GW scalar one has to solve the coupled Einstein and Klein-Gordon equations which come from the total action $S_{grav}^E + S_{GW}^E$ and impose the boundary conditions (3.2) and (3.5). This is in general a non-trivial task and exact analytic solutions can only be obtained in some particular cases [26]. The problem greatly simplifies if we can neglect the backreaction of the GW scalar on the $5D$ metric. In this case one simply has to solve the Klein-Gordon equation on the corresponding unperturbed gravitational background, provided by Eqs. (2.2) and (2.3), and this provides an approximate solution of the original coupled equations. In the RS case the actual value of μ (i.e. the position μ^{-1} of the IR brane) is the one which minimizes the value of the action on the corresponding solution. By plugging the solution into the action one gets, in addition to the vacuum energy term of Eq. (2.9), a potential $V_{GW}(\mu)$ for the radion whose minimum fixes the value of the (stabilized) modulus. The result is [25]

$$V_{GW}(\mu) = \epsilon v_0^2 k^4 + \mu^4 [(4 + 2\epsilon)(v_1 - v_0(\mu/k)^\epsilon)^2 - \epsilon v_1^2 + \delta T_1], \quad (3.6)$$

in the very good approximation of neglecting $(\mu/k)^4 \ll 1$.

For the potential (3.6) to have a (non-trivial) global minimum one must require

$$\begin{aligned} \text{for } \epsilon > 0, \quad & \frac{\delta T_1}{v_1^2} < \epsilon, \\ \text{for } \epsilon < 0, \quad & -(4 + \epsilon) < \frac{\delta T_1}{v_1^2} < \epsilon. \end{aligned} \quad (3.7)$$

If the previous conditions are satisfied the global minimum of $V_{GW}(\mu)$ is located at

$$\mu_{TeV} = k \left(\frac{v_1}{v_0} \right)^{1/\epsilon} X^{1/\epsilon}, \quad \text{where} \quad X = \frac{4 + \epsilon + \text{sign}(\epsilon) \sqrt{\epsilon(4 + \epsilon) - 4 \frac{\delta T_1}{v_1^2}}}{4 + 2\epsilon}. \quad (3.8)$$

It is also useful to have a formula for the value of the potential at its minimum. It is

$$V(\mu_{TeV}) = \epsilon v_0^2 k^4 + \mu_{TeV}^4 v_1^2 \frac{\epsilon}{2 + \epsilon} \left[\frac{\delta T_1}{v_1^2} - \text{sign}(\epsilon) \sqrt{\epsilon(4 + \epsilon) - 4 \frac{\delta T_1}{v_1^2}} \right]. \quad (3.9)$$

Equation (3.8) shows how the GW mechanism provides a solution to the Hierarchy Problem. Since k is associated to the Planck scale and μ_{TeV} to the Electroweak (TeV) one, an enormous fine-tuning is expected “a priori” in order to get μ_{TeV} out of microscopic parameters of order k . However by making a sensible choice of $|\epsilon|$ and v_1/v_0 not too far from 1 Eq. (3.8) can easily give rise to the required 16 orders of magnitude among μ_{TeV} and k . Solving the Hierarchy Problem is the greatest success of this class of models, and considering too high values of $|\epsilon|$ would spoil this success. If we at most allow for a two orders of magnitude hierarchy among v_1 and v_0 we get the upper bound:

$$|\epsilon| \lesssim \frac{1}{8}. \quad (3.10)$$

For $|\epsilon| = 1/20$, which is the reference value we will mostly use in the following, $v_1/v_0 \sim 10^{\text{sign}(\epsilon)4/5}$.

For the above manipulations to make sense the GW field must provide a small back-reaction on the metric. To ensure this condition, the contribution of the GW field to the energy-momentum tensor must be compared with the one coming from the bulk cosmological constant. This leads to the constraints

$$\begin{aligned} \frac{\pi^2 v_1^2}{N^2} &< \frac{3}{|\epsilon(4+\epsilon)| + \epsilon^2} \frac{1}{X^2} \left(\frac{\mu}{k}\right)^{2\epsilon}, \\ \frac{\pi^2 v_1^2}{N^2} &< \frac{3}{|\epsilon(4+\epsilon)| + \epsilon(4+\epsilon) - 4\frac{\delta T_1}{v_1^2}}, \end{aligned} \quad (3.11)$$

where the $|\epsilon(4+\epsilon)|$ term in the denominators comes from the fact that, depending on the sign of ϵ , the stronger constraint arises from the $T_{\mu\nu}$ or T_{zz} components of the 5D energy-momentum tensor T_{MN} . The small back-reaction condition also implies another constraint, which was considered in [25] and ignored in [15]. It comes from comparing the RS brane tension in Eq. (2.6) with the δT_1 term of Eq. (3.1). Remembering that the latter has been treated as a correction, we must impose

$$|\delta T_1| < 24(ML)^3 = \frac{3}{2\pi^2} N^2. \quad (3.12)$$

Depending on the sign of ϵ significantly different constraints on v_1/N arise. When ϵ is positive $(\mu/k)^{2\epsilon}$ is small and the first bound in Eq. (3.11) is the relevant one. The two bounds could only be comparable for very small values of ϵ . In the following we will however mainly be interested in negative ϵ . In this case the first bound in Eq. (3.11) is weak and the second bound becomes the relevant one. As for the latter v_1^2 drops from the second line of Eq. (3.11) one gets, noticing that $\delta T_1 < 0$

$$|\delta T_1| < 12(ML)^3 = \frac{3}{4\pi^2} N^2, \quad (3.13)$$

which is a factor of 2 stronger than Eq. (3.12). Considering Eq. (3.7), Eq. (3.13) can be converted into a bound on v_1 as

$$\frac{\pi^2 v_1^2}{N^2} < \frac{3}{4|\epsilon|}. \quad (3.14)$$

The above condition is always stronger than the one which comes from the first line of Eq. (3.11). Indeed, $(\mu/k)^{2\epsilon} > 1$ and it is possible to show, using Eq. (3.7), that X is smaller than one. We can then conclude that for $\epsilon < 0$ Eq. (3.14) is the only small-backreaction condition, although one should however account for the consistency conditions in Eq. (3.7).

Focusing on the negative ϵ case it is convenient to define the variables

$$\theta = \frac{4}{3} \frac{\pi^2 |\delta T_1|}{N^2}, \quad \nu = \frac{4}{3} \frac{\pi^2 |\epsilon| v_1^2}{N^2}. \quad (3.15)$$

The perturbativity constraint (3.13) and the consistency conditions (3.7) can respectively be expressed as

$$\theta < 1, \quad \nu < \theta < \frac{4 - |\epsilon|}{|\epsilon|} \nu. \quad (3.16)$$

As far as ϵ is small, the last inequality is substantially irrelevant and all our constraints can be expressed in terms of two parameters only.

In order to discuss how the GW field affects the deconfined (AdS-S) phase, following, we have to construct an “off-shell” version of the AdS-S geometry (2.3) by defining a “Hawking temperature” $T_h \equiv 1/(\pi z_h)$ and relaxing the regularity condition (2.4). A 4D field $T_h(x)$ is associated to the parameter T_h . Very much like the radion field $\mu(x)$ controls the position μ^{-1} of the IR brane in the RS phase, $T_h(x)$ controls the position z_h of the AdS-S black hole horizon. Differently from the radion, however, T_h has a potential even in the absence of the GW field. Having detuned the condition (2.4), indeed, the space develops a conical singularity which, once regularized with a suitable spherical cap, gives rise to a potential for T_h with a minimum at $T_h = \beta_h^{-1} (\simeq T$ for $T \ll k$). Taking also into account the GW contribution, the T_h potential [*i.e.* the deconfined (AdS-S) phase free-energy] is [13]

$$F_d(T_h, T) = E_0 + \frac{3\pi^2 N^2}{4} T_h^4 - \pi^2 N^2 T T_h^3 + \frac{3\pi^2 N^2}{8} \nu X^2 \left(\frac{\mu_{TeV}}{\pi T_h} \right)^{2|\epsilon|} T_h^4, \quad (3.17)$$

where we subtracted the vacuum energy term

$$E_0 = -V_{GW}(\mu_{TeV}), \quad (3.18)$$

in order to cancel the cosmological constant term [Eq. (3.6) at the minimum] of the confined (RS) phase. At small $|\epsilon|$ the above formulas reduce to

$$F_d(T_h, T) \simeq E_0 + \pi^2 N^2 \left[\frac{3}{4} \left(1 + \frac{\nu}{2} \right) T_h^4 - T T_h^3 \right], \quad (3.19)$$

with

$$E_0 = \frac{3N^2}{4\pi^2} \sqrt{(\theta\nu - \nu^2)|\epsilon|} \mu_{TeV}^4. \quad (3.20)$$

Notice that the above expansion holds for $|\epsilon|^{1/2} \ll 1$ and fails for $\theta \gg \nu$. In this approximation F_d has a minimum at

$$T_h^{min} = \frac{T}{1 + \nu/2}, \quad (3.21)$$

and the free-energy at the minimum is

$$F_d^{min}(T) = E_0 - \frac{\pi^2 N^2}{4} \frac{T^4}{(1 + \nu/2)^3}. \quad (3.22)$$

The introduction of the $T_h(x)$ field associated to the horizon position also permits to develop an intuitive understanding of how tunneling among the two vacua occurs [13]: starting in the AdS-S phase at $T_h = T_h^{min}$ the horizon starts to move away from the *UV* brane since T_h reaches 0. At this point the horizon has disappeared and the metric (2.3) reduces to the one of the infinite *AdS*₅ space, which coincides with the RS one (2.2) for $\mu = 0$. The *IR* brane now appears from infinity and μ grows from zero to its equilibrium value μ_{TeV} . The radion, in this schematization, is the only field of the RS phase which undergoes a variation during the tunneling process and it is only possible to justify this approximation (at a not too high temperature compared with μ_{TeV}) if the RS KK gravitons are significantly heavier than the radion. In this case it is energetically expensive for the KK fields to move and the transition can be studied in an effective theory for the radion alone. With the aim of checking that indeed $m_r < m_{KK} \sim \pi \mu_{TeV}$ in all our allowed parameter space, and for completeness, we report here the radion Lagrangian [27, 21, 14]

$$\mathcal{L}_r = \frac{3N^2}{2\pi^2} \frac{1}{2} (\partial_\nu \mu)^2 - V_{GW}(\mu) = \frac{3N^2}{2\pi^2} \frac{1}{2} [(\partial_\nu \mu)^2 - m_r^2 \mu^2 + \dots], \quad (3.23)$$

where

$$\begin{aligned} m_r^2 &= 2(2 + \epsilon)\nu (4X + 4\epsilon X - 2\epsilon X^2 - 4X^2) \mu_{TeV}^2 \\ &\simeq 8\sqrt{-\epsilon(\theta - \nu)}\nu \mu_{TeV}^2. \end{aligned} \quad (3.24)$$

Fig. 1 shows level curves of m_r/μ_{TeV} in the region of parameters allowed by Eq. (3.16), we see that the radion is always sufficiently light for our approach to the transition to be meaningful.

Introducing the SM fields, as we will do in the following, does not dramatically change the picture of the transition, we will however have to include a second light scalar, the Higgs field, on the RS side. The transition becomes, in principle, a problem of tunneling in a two-dimensional field space, which is numerically much more complicated than the standard one-dimensional one. We will argue, however, the Higgs contribution to the bounce to be negligible and studying the one-dimensional radion tunneling will be sufficient for our purposes.

We conclude this section by observing that small-backreaction is not at all necessary for the GW mechanism to work, as shown in [26]. As long as $|\epsilon|$ is sufficiently small the

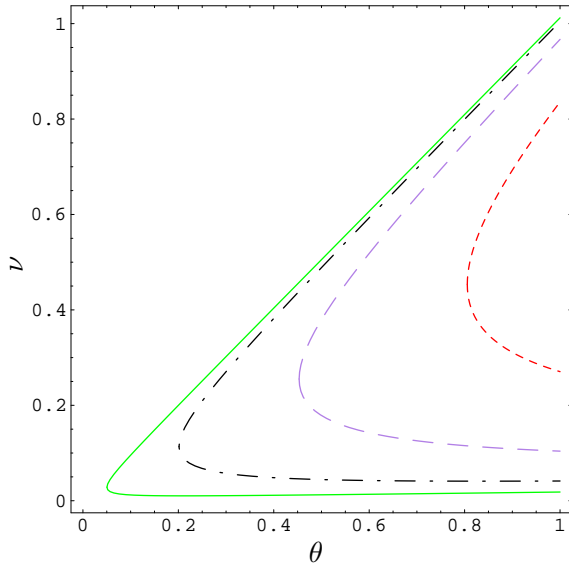


Figure 1: Level curves of m_r/μ_{TeV} equals to 0.8 (red short-dashed line), 0.6 (purple dashed), 0.4 (black dot-dashed) and 0.2 (green solid) in the plane (θ, ν) . We have fixed $\epsilon = -1/20$.

GW mechanism will still provide a solution to the Hierarchy Problem even in the presence of a significant backreaction. From this point of view the small backreaction conditions which we impose only have a *technical* motivation, as they ensure the consistency of our manipulations. All calculations done in this section could in principle be repeated taking backreaction into account. One should consider the coupled Einstein and Klein–Gordon equations, find the two solutions and substitute them back into the action. This would lead to exact expressions for the free energies of the two phases at leading order in N . For what concerns the dynamics of the phase transition, on the contrary small backreaction is more than a technical assumption. The point is that, as shown in Fig. 1 this condition ensures the radion to be light. If this were not the case, as previously discussed, the schematization of the transition by the radion tunneling would be meaningless and one would need to go to the true extra–dimensional gravitational instanton which connects the two vacua. This is most likely beyond the reach of our field–theoretical description of the two phases, as one should face the problem of describing in some way the process of the IR brane hitting the horizon and disappearing into the black–hole.

3.2 The Higgs field

Let us now introduce the Higgs field in our theory. As in the original RS scenario we take the Higgs doublet \bar{h} to be localized at the IR brane. The (Euclidean) action is then ⁴

$$S_{SM}^E = \int_{\partial\mathcal{M}_{IR}} \mathcal{L}_{SM}^E = \int d^4x \sqrt{\gamma^{IR}} \mathcal{L}_{SM}^E \quad (3.25)$$

where the Higgs doublet \bar{h} has a tree-level potential

$$V_0(\bar{h}, \bar{v}) = \lambda \left(\bar{h}^\dagger \bar{h} - \frac{1}{2} \bar{v}^2 \right)^2. \quad (3.26)$$

As for the rest of SM fields we will not consider a particular scenario although we will assume that gauge bosons and (at least part of) the SM fermions ⁵ are propagating in the bulk. We will just assume that the set of zero modes and localized fields at the minimum of the GW potential and for low enough energies (where all Kaluza-Klein excitations are decoupled) are described by the SM effective potential.

Using now the RS metric (2.2) one can write the action as

$$S_{SM}^E = \int d^4x \left\{ \left(\frac{\mu}{\mu_{TeV}} \right)^2 |D_\mu h|^2 + \left(\frac{\mu}{\mu_{TeV}} \right)^4 V_0(h, v) + \dots \right\} \quad (3.27)$$

where the Higgs field is redefined as

$$h = \frac{\mu_{TeV}}{k} \bar{h}, \quad \left[v = \frac{\mu_{TeV}}{k} \bar{v} \simeq 246 \text{ GeV} \right]. \quad (3.28)$$

Notice that Higgs fields and mass parameters [or vacuum expectation values], are red-shifted with a power of the factor μ_{TeV}/k according to their dimension.

The IR brane terms only contribute to the RS phase and hence, in the present model, the Higgs field is not present at all in AdS-S. The holographic reason for this is that the Higgs particles ⁶ are entirely composite objects which cannot be present in the deconfined high-temperature plasma.

Including the contribution from light SM fields the AdS-S free energy becomes

$$F_d = E_0 - \frac{\pi^2 N^2}{4} \frac{T^4}{(1 + \nu/2)^3} - \frac{\pi^2}{90} g_d^* T^4 \quad (3.29)$$

and the RS free-energy is

$$F_c(\mu, \phi_c, T) = V_{RS}(\mu, \phi_c, T) + E_0 - \frac{\pi^2}{90} g_c^* T^4, \quad (3.30)$$

⁴We are assuming here for simplicity that there is no Higgs-radion mixing from a term like $\xi \int d^4x \sqrt{\gamma^{IR}} R(\gamma^{IR}) \bar{h}^\dagger \bar{h}$, i.e. that $\xi \simeq 0$.

⁵Some fermions could also be localized in the IR brane as the Higgs fields.

⁶As well as other particles possibly localized on the IR brane.

where $g_c^* \sim 100$ (g_d^*) is the effective number of light SM degrees of freedom in the RS (AdS-S) phase, $\phi_c \equiv \sqrt{2}h^0$ and $V_{RS}(\mu, \phi_c, T)$ indicates the radion-Higgs potential. At the tree-level it reads

$$V_{RS}(\mu, \phi_c) = V_{GW}(\mu) + \left(\frac{\mu}{\mu_{TeV}}\right)^4 \frac{\lambda}{4}(\phi_c^2 - v^2)^2 \quad (3.31)$$

As we can see from Eq. (3.31) the typical size of the SM potential is $V_{SM} \sim v^4$ while that of the GW potential is much larger, i.e. $V_{GW} \sim \mu_{TeV}^4$. Therefore the total potential

$$V_{RS} = V_{GW} [1 + \mathcal{O}(v^4/\mu_{TeV}^4)] \quad (3.32)$$

can be approximated, as far as the phase transition from AdS-S to RS is concerned, by the GW radion potential. In fact at the typical radion transition temperatures the SM potential is a little perturbation of the radion potential and should not alter the bounce solution and the corresponding Euclidean action that governs the phase transition. The radion potential then produces a supercooling of the system and the electroweak phase transition (EWPT) takes place at much lower temperatures than the typical EWPT ones and makes it to be much stronger. We postpone the numerical analysis of this behaviour to section 5.

In the approximation of Eq. (3.31) the free energy is minimized for $\mu = \mu_{TeV}$ and $\phi_c = v$, and at the minimum

$$F_c^{min}(T) = -\frac{\pi^2}{90} g_c^* T^4. \quad (3.33)$$

Although irrelevant for what concerns the radion-phase transition, one-loop corrections to the Higgs potential are important at high enough temperatures to determine the VEV of the Higgs field. For $\mu = \mu_{TeV}$ we are able to compute the one-loop Higgs potential as we have assumed that low energy dynamics is just the SM one.

In the \overline{MS} -scheme the one-loop Coleman-Weinberg potential depends on the renormalization scale Q through the ratio m_i^2/Q^2 while the thermal corrections similarly depend on the temperature through the ratio m_i^2/T^2 . We can then write the SM potential at $\mu = \mu_{TeV}$ as

$$\begin{aligned} V_{SM} &= \frac{\lambda}{4} (\phi_c^2 - v^2)^2 + \frac{1}{64\pi^2} \sum_{i=W,Z,h,\chi,t} n_i [m_i(\phi_c)]^4 \left[\log \frac{[m_i(\phi_c)]^2}{Q^2} - C_i \right] \\ &+ \frac{T^4}{2\pi^2} \left[\sum_{i=W,Z,h,\chi} n_i J_B[m_i^2/T^2] + n_t J_F[m_t^2/T^2] \right] \end{aligned} \quad (3.34)$$

where the thermal fermionic (bosonic) function $J_{F(B)}$ are given by

$$J_{F(B)}(y^2) = \int_0^\infty dx \, x^2 \log \left[1 \pm e^{-\sqrt{x^2+y^2}} \right], \quad (3.35)$$

the constants C_i derive from the $\overline{\text{MS}}$ renormalization scheme we have used, and n_i are the degrees of freedom of the i field, that is

$$\begin{aligned} C_W = C_Z = \frac{5}{6} \quad C_h = C_\chi = C_t = \frac{3}{2} \\ n_W = 6, \quad n_Z = 3, \quad n_h = 1, \quad n_\chi = 3, \quad n_t = -12, \end{aligned} \quad (3.36)$$

The only fermion that contributes sizeably to the effective potential for $\phi_c \neq 0$ is the top quark t since the other fermions are very weakly coupled to the Higgs doublet. For practical purposes we fix $Q = m_t(v)$ which is nearby the Higgs VEV. As for the thermal corrections it could have been possible to use a better approximation including plasma effects [28]-[35], however we think that for the purposes of the present paper the one-loop approximation is good enough.

4 The Phase Transition

At high temperatures (early times) a deconfined (strongly-coupled) plasma fills the Universe, which is described by the Friedmann–Robertson–Walker metric $ds^2 = dt^2 - a^2(t)d\vec{x}^2$ and expands according to the Friedmann equation

$$\frac{\dot{a}}{a} = H = \sqrt{\frac{8\pi}{3M_P^2}\rho_d}, \quad (4.1)$$

where ρ_d is the energy density of the plasma and could be easily extracted from the free-energy in Eq. (3.29). As the Universe expands, it cools down and a confining phase transition can occur when the free-energy of the deconfined phase equals the confined one. This happens at a critical temperature T_c which is obtained by equating Eqs. (3.29) and (3.33):

$$T_c^4 = 3\sqrt{(\theta\nu - \nu^2)|\epsilon|} \left[\frac{1}{(1 + \nu/2)^3} - \frac{2\Delta g^*}{45N^2} \right]^{-1} \left(\frac{\mu_{TeV}}{\pi} \right)^4. \quad (4.2)$$

where $\Delta g^* = g_c^* - g_d^*$ and g_d^* is the number of light degrees of freedom in the AdS-S phase that equals, in the model we are considering, to the Higgsless SM degrees of freedom. At small enough N and large enough ν , T_c^4 can become negative. This is due to the fact that the T^4 term in Eq. (3.33) becomes larger than the one in Eq. (3.29) and in this case, given that E_0 is positive, the deconfined phase is never stable, the Universe stays forever in the confined one and no phase transition occurs. However for $N \geq 3$, and using $\Delta g^* = 4$ in our model, this situation is avoided provided that the constraints (3.16) are fulfilled. In most of the allowed parameter space the critical temperature is a bit smaller than μ_{TeV} : $T_c \sim \mu_{TeV}/\pi$.

4.1 Completion of the transition

Formally, the phase transition begins as soon as the temperature drops below T_c . It will then be convenient, to fix ideas, to choose the origin of time as $T(0) = T_c$ and rescale

the space coordinates so that $a(0) = 1$. There is a simple one-to-one relation among temperature and time, $T(t) = T_c/a(t)$ and, using Eq. (4.1)

$$\dot{T} = -TH(T) = -\frac{T}{M_P} \sqrt{\frac{8\pi}{3}} \rho_d(T). \quad (4.3)$$

For $T < T_c$ there is a non-zero probability for bubbles of the confined phase to form, the rate of bubble nucleation for unit physical volume can be expressed as

$$\lambda(T) = A(T) e^{-S(T)}, \quad (4.4)$$

where the exponential suppression is due to semiclassical tunneling and the bounce action $S(T)$ will be computed in the following. The prefactor A can be estimated on dimensional grounds, $A \sim T^a T_c^b$ with $a + b = 4$. In particular for very low temperatures, as those that will be found in this work, $a = 0, b = 4$. The nucleation rate is dominated by the exponential so that this rough estimate of the prefactor will be sufficient for our purposes.

To have an idea of how fast the transition proceeds we follow [36] and write down the probability that one point of space remains in the old (deconfined) phase at the time t . Assuming the bubble expands at the speed of light

$$\begin{aligned} p &= \exp \left[-\frac{4\pi}{3} \int_0^t dt_1 a^3(t_1) \lambda(T(t_1)) \left(\int_{t_1}^t dt_2 \frac{1}{a(t_2)} \right)^3 \right] \\ &= \exp \left[-\frac{4\pi}{3} \int_T^{T_c} dT_1 \frac{\lambda(T_1)}{T_1^4} \left(\frac{M_P}{\sqrt{8\pi/3}} \right)^4 \frac{1}{\sqrt{\rho_d(T_1)}} \left(\int_T^{T_1} dT_2 \frac{1}{\sqrt{\rho_d(T_2)}} \right)^3 \right], \end{aligned} \quad (4.5)$$

where we used Eq. (4.3) to change variable in the time integrals. The nucleation rate, due to the exponential factor in eq. (4.4), undergoes exponential variation in the course of time, *i.e.* temperature, so that there could be regions of temperature in which the dT_1 integral in Eq. (4.5) only receives negligible contributions. Using dimensional analysis (we are considering now $T \sim T_c \sim TeV$) to estimate ρ_d and the dT_2 integral in Eq. (4.4) (which we could as well compute using Eq. (3.29) without changing the result which follows) we get that the region of temperatures for which

$$S(T) > B \equiv 4 \log \left(\frac{M_P}{\mu_{TeV}} \right) \approx 148 \Rightarrow \left[\frac{\lambda(T)}{T^4} \left(\frac{M_P}{T} \right)^4 \ll 1 \quad \text{for } T \sim 1 \text{ TeV} \right], \quad (4.6)$$

cannot contribute appreciably to the integral if T is not orders of magnitude smaller than $\mu_{TeV} \sim TeV$.

We will soon see that, for $T \simeq T_c$, the condition (4.6) is always fulfilled in the case we are considering, so that the phase transition does not effectively start at $T = T_c$. As discussed above, it is very unlikely to find a point in the new phase, the Universe is filled by a supercooled deconfined plasma and keeps expanding with the energy density associated to Eq. (3.29). It is worth remarking that, as the temperature drops below

$$T_i^4 = \sqrt{(\theta\nu - \nu^2)|\epsilon|} (1 + \nu/2)^3 \left(\frac{\mu_{TeV}}{\pi} \right)^4 < T_c^4/3, \quad (4.7)$$

the cosmological constant starts to dominate over radiation and an inflationary epoch begins. The total number of e-folds of inflation is $\sim \log T_i/T_n$ where T_n , to be defined below, is the temperature at which the transition effectively occurs. In the inflationary epoch we can use $\rho_d = E_0$ in Eq. (4.5) and write down more explicitly the probability of transition as

$$p(T) = \exp \left[-\frac{4\pi}{3} \int_T^{T_i} \frac{dT_1}{T_1} \frac{\lambda(T_1)}{E_0^2} \left(\frac{M_P}{\sqrt{8\pi/3}} \right)^4 \left(1 - \frac{T}{T_1} \right)^3 \right], \quad (4.8)$$

where we neglected the $[T_i, T_c]$ part of the integral. Once again we can check that temperatures for which the condition (4.6) holds do not contribute to the integral. In our model, the bounce action $S(T)$ monotonically decreases with temperature so that if **(a)** $S(T \rightarrow 0) > B$ the action never crosses the critical value while if **(b)** $S(T \rightarrow 0) < B$ we can define the nucleation temperature T_n as

$$S(T_n) = B. \quad (4.9)$$

The case **(a)** corresponds to the “slow” phase transition considered in [37] and, despite of the fact that the probability (4.8) will eventually go to zero, bubbles will not percolate, the phase transition will never end and we will have an empty and cold Universe. Avoiding **(a)** will give us a strong constraint on the allowed parameter space of the model and, in particular, on the maximum value of the number of colors N .

Let us now focus on case **(b)**. For $T_1 = T_i$ the nucleation rate is always too small for the transition to start but for $T_1 = T_n$ the argument of the integral in Eq. (4.8) becomes of order one. It is important to remark that the bounce action has a power-like behaviour with temperature so that the rate grows exponentially. When the temperature crosses T_n the argument of the integral suddenly passes from being much smaller to much bigger than one. The integral suddenly becomes large, the probability goes to zero and the phase transition ends. During the time the phase transition lasts, therefore, the Universe undergoes a negligible cooling, *i.e.* a negligible expansion. On the scale of the evolution of the Universe the phase transition is instantaneous: bubbles expand, collide and percolate as if the Universe were static.

We can illustrate this behaviour with a simple toy model. Since the integral (4.8) is dominated by temperatures very close to T_n one can assume that the action in (4.4) behaves linearly with T , *i.e.* $S(T/T_n) = \alpha + \beta T/T_n$ where $\alpha + \beta \sim B$ is the condition (4.9) and the slope β has been computed numerically and yields values $\beta \sim 50 - 100$ (depending on the values of the GW parameters). We can then write for the probability (4.8) the expression

$$p(T) = \exp \left[-\frac{4\pi}{3} \int_T^{T_i} \frac{dT_1}{T_1} e^B e^{-(\alpha + \beta T_1/T_n)} \left(1 - \frac{T}{T_1} \right)^3 \right]. \quad (4.10)$$

The behaviour of the probability $p(T)$ is shown in the left panel of Fig. 2. We see that, in

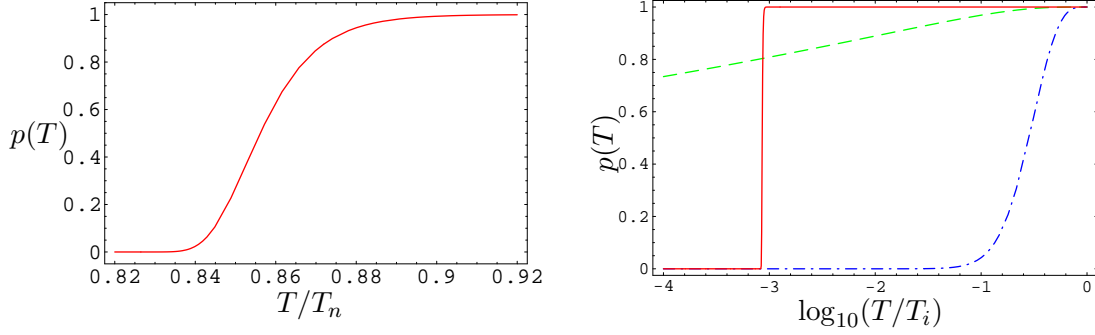


Figure 2: Left panel: Plot of the probability (4.10) as a function of T/T_n for $T_n = 10^{-3}T_i$ and a slope $\beta = 100$. Right panel: Comparison of the previous plot [red (solid) line] as a function of $\log_{10} T/T_i$ with the probability (4.11) for $\epsilon_0 = 1$ [blue (dot-dashed) line] and $\epsilon_0 = .01$ [green (dashed) line].

this particular case the phase transition happens between $T = 0.88 T_n$ and $T = 0.84 T_n$, a negligible cooling that corresponds to the little expansion of 0.05 e-folds during the phase transition. The model considered in Ref. [37] corresponds to the case where $\beta = 0$ and Eq. (4.10) reads

$$p(T) = \exp \left[-\frac{4\pi}{3}\epsilon_0 \left(N_e - \frac{11}{6} + 3e^{-N_e} - \frac{3}{2}e^{-2N_e} + \frac{1}{3}e^{-3N_e} \right) \right] \quad (4.11)$$

where $\epsilon_0 = \exp(B - \alpha)$ and we can see that a large number of e-folds $N_e(T) = \log(T_i/T)$ is related to the value of ϵ_0 by $N_e \sim 3/4\pi\epsilon_0$ which would imply $\epsilon_0 \ll 1$. On the other hand for $\epsilon_0 \sim 1$ we obtain $p \ll 1$ after an $\mathcal{O}(1)$ number of e-folds of inflation. This does not happen in our case since nucleation is triggered by the temperature T_n where condition (4.9) holds. The difference between both situations is illustrated in the right panel of Fig. 2.

Finally, as it was discussed in Ref. [38] two conditions must be satisfied by $\gamma \equiv \lambda/H^4$ to complete the phase transition in an (inflationary) first-order phase transition. **i)** $\gamma > 9/4\pi$ is required for percolation; **ii)** $\gamma \simeq 0$ for almost all the inflationary period, otherwise bubbles are formed, grow during inflation and distort the CMB radiation. We have checked that in our model both conditions are satisfied at least for moderate number of e-folds of inflation, *i.e.* for $N_e \leq 6$. Certainly condition **i)** is satisfied since γ crosses from values larger to values smaller than one around the nucleation temperature. Condition **ii)** is also satisfied since H is a constant during the inflationary period while Γ varies exponentially with the temperature so that γ varies very quickly near the nucleation temperature. Therefore big bubbles do not have the chance to develop. We did not make the numerical analysis for the very small values of the nucleation temperature corresponding to the number of e-folds of inflation consistent with the required amount of cosmological inflation ($N_e \sim 30$) because inflation was not the main issue in this paper. We will come back to

this issue in a different work.

The new-phase plasma thermalizes and the expansion continues with the free-energy given by Eq. (3.30). During the transition, of course, the energy (or what is the same, given that the Universe is static, the energy density) must be conserved so that the Universe will end up in the confined phase with a “reheating” temperature T_R given by

$$\frac{\pi^2}{30} g_c^* T_R^4 = E_0. \quad (4.12)$$

To obtain the above equation we equated $\rho_c(T_R)$ obtained from Eq. (3.30) with $\rho_d(T_n)$ and neglected the nucleation temperature $T_n \ll T_i$.

4.2 Bubble nucleation: approximate analytical results

We will now describe in detail the phase transition from the deconfined (AdS-S) to the confined (RS) phase as described by the respective free-energies given by Eqs. (3.17) and (3.30). At the critical temperature T_c the two minima are degenerate and thus the Euclidean action $S(T_c) \rightarrow \infty$. Below T_c the first bubbles that can be formed are those with $O(3)$ symmetry, thin walls and very large radii. In this case the probability of bubble formation is governed by $S = S_3(T)/T$ where S_3 is the Euclidean action with $O(3)$ symmetry. In the thin wall approximation the action can be given an analytic expression as $S_3 = 16\pi S_1^3/3(\Delta V)^2$ where S_1 is the surface tension that can be evaluated in the limit $T \rightarrow T_c$ and ΔV is the depth of the true vacuum relative to the false one. Using the analytic approximation we will prove now that the radion phase transition will not allow the formation of thin wall bubbles. For that we will momentarily forget the Higgs field since its presence will not alter the following conclusions. A straightforward application of the thin wall formula for the deconfinement/confinement radion phase transition leads to

$$\frac{S_3(T)}{T} \simeq \frac{64\pi}{3} \frac{\mu_{TeV}^2}{\sqrt{2E_0}} \left(\frac{3N^2}{2\pi^2} \right)^{3/2} \frac{\mu_{TeV}/T}{(1 - T^4/T_c^4)^2} \quad (4.13)$$

where E_0 is the vacuum energy defined in (3.20). Eq. (4.13) shows that $S_3(T)/T$ goes to infinity in both limits $T \rightarrow 0$ and $T \rightarrow T_c$. The function $S_3(T)/T$ has in fact a minimum (that corresponds to the maximal probability of nucleation) at $T^* = T_c/\sqrt{3}$. Using now the relation (4.2) between μ_{TeV} and T_c one can write the final expression for the action (4.13) at $T = T^*$ as

$$\frac{S_3(T^*)}{T^*} \simeq \frac{50N^2}{[(\theta - \nu)\nu|\epsilon|]^{3/8}} \left[\frac{1}{(1 + \nu/2)^3} - \frac{2\Delta g^*}{45N^2} \right]^{1/4} > \frac{50N^2}{|\epsilon|^{3/8}} \quad (4.14)$$

where the last inequality follows from the fact that the term raised to the power 1/4 is an order one number and from the perturbativity bounds $\theta < 1$, $\nu < 1$. For instance for $|\epsilon| \sim 1/10$, S_3/T does not satisfy condition (4.9) for $N \geq 2$. We can observe that if the

values of the parameters (θ, ν) are small, as it corresponds to the perturbativity region, the values of the Euclidean action S_3/T can be huge.

Of course thin wall bubbles with symmetry $O(4)$ have Euclidean actions larger than those just described with $O(3)$ symmetry. On the other hand since there is supercooling we have found that in most of the available parameter space the least action corresponds to $O(4)$ symmetric solutions.

For $O(4)$ symmetric bubbles we have worked out the thick wall approximation that we will illustrate now and where we have also included the Higgs potential. In order to do that we will work out the thick wall approximation for a set of field with (in general) non-canonical kinetic terms as follows.

We will then consider a theory with a number of scalar fields $\phi \equiv (\phi_1, \phi_2, \dots)$ with a potential $V(\phi)$ and general non-canonical kinetic functions $f_i(\phi)$. The euclidean action for $O(4)$ configurations can be written as

$$S_4 = 2\pi^2 \int_0^\infty d\rho \rho^3 \left(\sum_i f_i(\phi) \frac{1}{2} \phi_i'^2 + V(\phi) \right) \quad (4.15)$$

where we are using the notation $\phi' = d\phi/d\rho$. The potential V has a false vacuum (say at $\tilde{\phi} = 0$) where the energy is normalized to be zero $V(\tilde{\phi}) = 0$ and a true minimum at $\phi = \phi_0$. The bounce solution for $O(4)$ symmetric bubbles is obtained by solving the equations of motion (EOM)

$$f_i \phi_i'' + \frac{3}{\rho} f_i \phi_i' + \phi_j' \frac{df_i}{d\phi_j} \phi_i' = \frac{dV}{d\phi_i} + \frac{1}{2} \frac{df_j}{d\phi_j} \phi_j'^2, \quad \text{no summation on } i \quad (4.16)$$

with the boundary conditions $\phi'(\rho = 0) = 0$ and $\phi(\rho \rightarrow \infty) = \tilde{\phi}$.

We can now consider a bubble of true vacuum and radius R inside an exterior of false vacuum. Since the potential outside the bubble is zero and the ϕ -profile constant, only the region inside the bubble will contribute to the action (4.15). If $\phi^* \equiv \phi(0)$ is the value of ϕ at which the bounce starts ⁷, $\delta\phi = \phi^* - \tilde{\phi}$ is the total variation of ϕ inside the bubble wall δR ⁸. We can then approximate the action (4.15) by

$$S_4 \simeq \pi^2 R^3 \sum_i f_i \left(\frac{\delta\phi_i}{\delta R} \right)^2 \delta R + \frac{\pi^2}{2} \bar{V} R^4 \quad (4.17)$$

where $\bar{V} < 0$ is a suitable average of the potential inside the bubble. We will take $\bar{V} = V(\phi^*)$ and will use the notation $V(\phi^*) \equiv V^*$ and so on. Notice that in this way we will underestimate the bounce action.

If the bubble is thick we take $\delta R = R$ and determine the radius R_c of the bubble by extremizing Eq. (4.17) with respect to R . This gives for the critical radius

$$R_c^2 = \frac{\sum_i \phi_i^{*2} f_i^*}{-V^*} \quad (4.18)$$

⁷Notice that ϕ^* does not coincide with ϕ_0 .

⁸The bubble wall δR is defined as the region ρ where ϕ varies.

and for the critical action

$$S_4(R_c) = \frac{\pi^2}{2} \frac{(\sum_i \phi_i^{*2} f_i^*)^2}{-V^*} \quad (4.19)$$

We will apply the previous expressions to the case of the system of two fields, radion and Higgs fields, (μ, ϕ_c) with non-canonical kinetic functions

$$\mathcal{L}_{kin} = \frac{3N^2}{2\pi^2} \frac{1}{2} (\partial_\nu \mu)^2 + \frac{\mu^2}{\mu_{TeV}^2} |\partial_\nu h|^2 \quad (4.20)$$

and potential

$$V \equiv \mu^4 \left(\mathcal{V}_{GW} + \frac{\mathcal{V}_{SM}}{\mu_{TeV}^4} \right) \quad (4.21)$$

where ⁹

$$\begin{aligned} \mathcal{V}_{GW}(\mu) &= (4 + 2\epsilon) \left[v_1 - v_0 \left(\frac{\mu}{k} \right)^\epsilon \right]^2 + \delta T_1 - \epsilon v_1^2 \\ \mathcal{V}_{SM}(\phi_c) &= \frac{1}{4} \lambda (\phi_c^2 - v^2)^2 \end{aligned} \quad (4.22)$$

The value of the critical action is then given by

$$S_4 = \frac{\pi^2}{2} \frac{\left(\frac{3N^2}{2\pi^2} + \frac{\phi_c^{*2}}{\mu_{TeV}^2} \right)^2}{-\mathcal{V}_{GW}^* - \mathcal{V}_{SM}^*} \quad (4.23)$$

which depends on the values of μ^* and ϕ_c^* that in turn do not necessarily coincide with their vacuum values μ_{TeV} and v respectively. In fact the precise values of $\mu^* = \mu(0)$ and $\phi_c^* = \phi_c(0)$ require of a numerical calculation of the bounce solution. Here we just want to give a plausibility argument for the phase transition to happen.

The phase transition should happen when $S_4 \sim B$ as we have seen in (4.9). The actual value of S_4 in Eq. (4.23) depends, for fixed values of the GW potential parameters, on the fields μ^* and ϕ_c^* . We can minimize the action S_4 with respect to those fields in order to obtain the most favorable configuration for the bounce solution. Minimization with respect to μ^* yields the value

$$\mu^* = k \left(\frac{v_1}{v_0} \right)^{1/\epsilon} \quad (4.24)$$

for which the thick-wall action is found to be

$$S_4(\phi_c^*) = \frac{\pi^2}{2} \frac{\left(\frac{3N^2}{2\pi^2} + \frac{\phi_c^{*2}}{\mu_{TeV}^2} \right)^2}{\epsilon v_1^2 - \delta T_1 - \mathcal{V}_{SM}^*} \quad (4.25)$$

The action (4.25) has a minimum at $\phi_c^* = 0$ for light Higgs masses. However the point $(\mu^*, 0)$ is a saddle point of the potential and the corresponding configuration is classically

⁹For the purpose of this section it is enough to just consider the tree level SM potential with radiatively corrected parameters.

stable. This situation is avoided for values of $\phi_c^* \neq 0$. Since the function $S_4(\phi_c^*)$ is monotonically increasing between $\phi_c^* = 0$ and $\phi_c^* = v$ a conservative assumption would be to fix $S_4(v) < B$ and therefore this condition will be satisfied by all configurations with $0 < \phi_c^* \leq v$. The $S_4(v) < B$ condition can be expressed as

$$\theta - \nu > \frac{3N^2}{2B} \left(1 + \frac{2\pi^2}{3N^2} \frac{v^2}{\mu_{TeV}^2} \right)^2 \simeq \frac{3N^2}{2B} \left(1 + \frac{0.4}{N^2} \right)^2 \quad (4.26)$$

where the second term inside the squared is a very tiny correction reflecting the fact that the SM potential is a small perturbation of the GW potential.

4.3 Bubble nucleation: numerical results

Generally speaking, the approximation methods used in the previous section are barely reliable. The main limitation is that they do not provide a reliable determination of the nucleation temperature as it is not possible to know, a priori, which shape (thick or thin) the bounce solution has at a given temperature. A numerical calculation of the bounce is therefore needed, and in the case of a single scalar field the solution can be easily found iteratively by the technique of over-shoots and under-shoots¹⁰. Clearly this can be done at zero and finite temperature.

In our case we have three fields (T_h , μ and h) involved in the bounce but, as we have discussed before, the Higgs does contribute to the bubble action with a tiny amount. Moreover the two remaining fields follow a single path in the two-dimensional field configuration space [13] and then we can consider the transition for a single field defined as

$$\Phi \equiv \begin{cases} -\left(N\sqrt{3/2}/\pi\right) T_h & \text{for } \Phi < 0 \\ \left(N\sqrt{3/2}/\pi\right) \mu & \text{for } \Phi > 0, \end{cases} \quad (4.27)$$

which has a canonical kinetic term¹¹ and the potential¹²

$$V(\Phi, T) = F_d \left(\pi\sqrt{2/3}/N \Phi, T \right) \Theta(-\Phi) + F_c \left(\pi\sqrt{2/3}/N \Phi, 0, T \right) \Theta(\Phi) \quad (4.28)$$

where Θ is the Heaviside step function.

Figure 3 provides an example of the numerical results we find for the bounce action [$S = S_4$ or $S = S_3/T$] with $O(3)$ and $O(4)$ symmetry in two typical points of our parameter space of $N = 3$. The comparison with analytical (thick and thin) formulas shows up a considerable discrepancy. The nucleation rate, at a given temperature, is dominated by the bounce of minimal action and, depending on the point in the parameter space, bounces

¹⁰We have explicitly checked our bounce program for the potentials of Ref. [39]

¹¹We are supposing for T_h the kinetic term $\frac{3N^2}{2\pi^2} \frac{1}{2} (\partial_\nu T_h)^2$ similar to the radion one.

¹²This potential is a simplification of that considered in the numerical analysis. Since for $T \neq 0$ the potential is discontinuous at $\Phi = 0$, it has been regularized and checked that the result is not sensitive to the regularization.

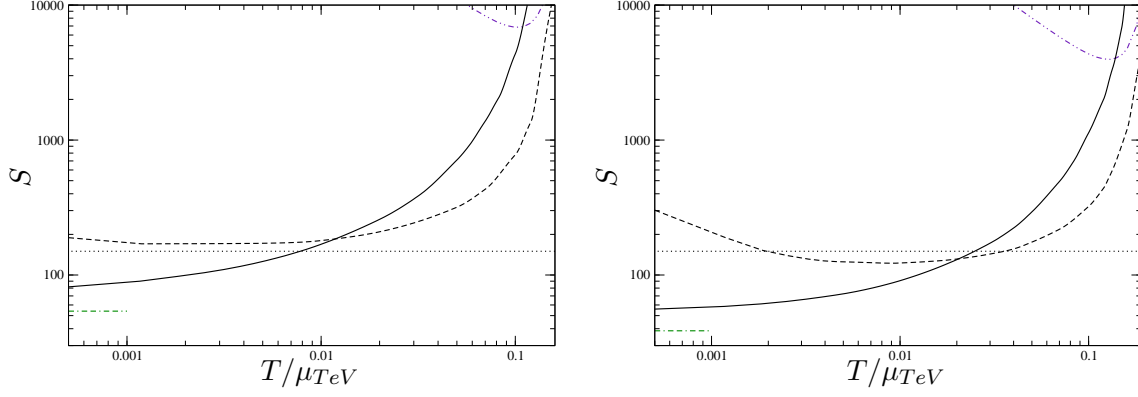


Figure 3: Solid [dashed] lines is the plot of the $O(4)$ [$O(3)$] Euclidean action as a function of T/μ_{TeV} for $N = 3$, $\epsilon = -1/20$ and, for the left [right] panel, $(\theta, \nu) = (0.35, 0.1)$ [$(\theta, \nu) = (0.6, 0.25)$]. On the left [right] the transition occurs via $O(4)$ [$O(3)$] bubbles. The analytical thin wall $O(3)$ (4.14) is plotted in double-dotted-dashed and the $O(4)$ analytical asymptotic value (4.25) in double-dashed-dotted.

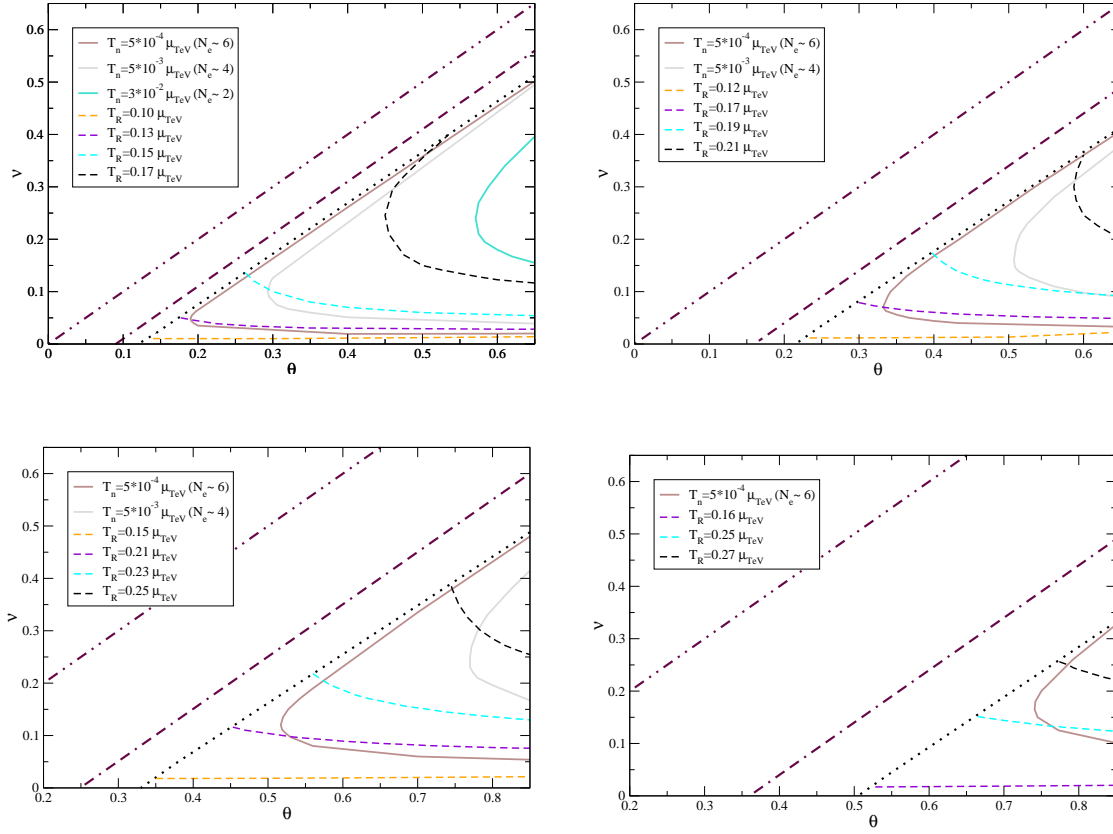


Figure 4: Plot of the allowed regions in the plane (θ, ν) for $N = 3$ (upper-left panel), $N = 4$ (upper-right panel), $N = 5$ (lower-left panel) and $N = 6$ (lower-right panel), with $\epsilon = -1/20$ and v_0 as a function of μ_{TeV} . The consistency bound $\theta < \nu$ is marked by a double-dotted-dashed line. The region where the nucleation is on the right of the dotted line, obtained by numerical $O(4)$ bubbles at $T_n = 0$. The same upper bound, but calculated using analytical approximations, is the double-dashed-dotted line. The points where the nucleation occurs at some fixed temperature are indicated by colored solid lines. Finally, several reheating temperature curves are drawn in dashed.

with either symmetries can be dominant. In all cases, however, the nucleation temperature is quite small. For the cases with a moderate number of e-folds ($N_e \leq 6$) that we have analyzed numerically we have checked that the slope of the Euclidean action $S(T/T_n)$ is $\beta \sim 50 - 100$ as it was anticipated in section 4.1.

Most of our numerical results are summarized in Fig. 4 which shows, for $\epsilon = -1/20$ and different values of N , the triangle in the θ - ν plane allowed by consistency (3.16) and, inside that, the analytic bound for the nucleation to happen as obtained by Eq. (4.26). Contour plots are shown for fixed nucleation temperature $T_n = 5 \cdot 10^{-4} \mu_{TeV}$, $T_n = 5 \cdot 10^{-3} \mu_{TeV}$ and $T_n = 5 \cdot 10^{-2} \mu_{TeV}$, corresponding to an inflation of $N_e \sim 6, 4, 2$, respectively. Regions of higher nucleation temperature, *i.e.* smaller inflation, are to the right of such level curves. As we can see in the allowed region a supercooling is necessary before permitting nucleation, and the larger N the lower T_n as predicted by the analytical approximations. In the allowed area, $O(4)$ bubbles dominate over $O(3)$, except in the case $N = 3$ when $T_n \gtrsim 10^{-2} \mu_{TeV}$. At $T = 0$ the GW potential, for $\epsilon < 0$, has a local minimum at $\mu = 0$ and zero-temperature nucleation occurs as a tunneling from this secondary minimum to the global one. In this way we numerically obtained (dotted line in the Fig. 4) the region in which nucleation is allowed. We see that the analytical formula provides a reasonable approximation. Also in Fig. 4 level contours for fixed values of the reheating temperature in units of μ_{TeV} (dashed lines) are shown.

Until now we have considered $O(4)$ solutions also at finite temperature, but strictly speaking they have sense only if the diameter of the bubble $2R$ is smaller than T_n^{-1} , the size of the compactified dimension at the nucleation temperature. Under that circumstance $O(4)$ is a good approximate symmetry [39]. To show that explicitly we plot in Fig. 5 the nucleation temperature T_n (without considering $O(3)$ solutions) and the corresponding $T_{lim} \equiv 1/(2R)\mu_{TeV}$ as a function of θ along the bisectrix [$\nu = \theta/2 - 1/20$] of the allowed region of Fig. 4 for $N = 3$ ¹³. The restriction of this analysis to the bisectrix in $N = 3$ is justified by the fact that along this path the maximal nucleation temperatures are reached and therefore it should be the worse region for the $O(4)$ approximate symmetry. Finally, from the plot we can conclude *a posteriori* that $O(4)$ actions considered in Fig. 4 make sense.

5 Conditions for electroweak baryogenesis

As we have seen the electroweak phase transition in the RS model, triggered by the radion phase transition, is a strong (supercooled) first-order one. This is unlike the pure Standard Model where the electroweak phase transition is very weakly first order at any perturbative level¹⁴. Since the weakness of the electroweak phase transition in the Standard Model was one of the main obstacles to the mechanism of electroweak baryogenesis we can see

¹³R is calculated using the $O(4)$ thick wall approximation.

¹⁴In fact non-perturbative analyses have shown that it is so weak that it disappears (it becomes a continuous crossover) when non-perturbative effects are taken into account.

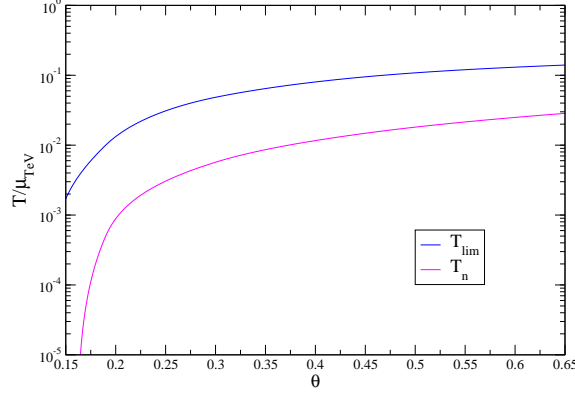


Figure 5: Lower curve: Plot of T_n/μ_{TeV} as a function of θ along the bisectrix $[\nu = \theta/2 - 1/20]$ of the allowed region in the upper-left plot of Fig. 4 ($N = 3$). Upper curve: Similar plot for $T_{lim} \equiv 1/(2R)\mu_{TeV}$ where R is the radius of the $O(4)$ bubble in the thick wall approximation.

that the situation is completely different in the Randall-Sundrum setup.

The first condition to be imposed is the non-erasure of the generated baryon asymmetry at the nucleation temperature inside the bubbles. As we can easily check this does not really impose any additional condition on the model parameters. In fact because the phase transition is strongly first order, and in particular $\langle \phi_c(T_n) \rangle / T_n \gg 1$, sphalerons are totally inactive inside the bubbles and the baryon asymmetry generated by some extra source of CP -violation (on top of the standard CKM phase) will not be erased in the broken phase.

The second condition that is required is that sphalerons be active outside the bubbles, as they are in the pure Standard Model. In the symmetric phase, outside the bubbles, the sphaleron rate can be computed from dimensional grounds [40] as $\Gamma_{sph} \sim \kappa \alpha_W^4 T^4$ where the coefficient κ has been evaluated numerically in [41] with the result $0.1 \leq \kappa \leq 1$ and α_W is the weak gauge coupling constant. The rate of baryon number non-conserving processes $V_B(T)$ is related to Γ_{sph} by [42]

$$V_B(T) = \frac{13}{2} N_f \frac{\Gamma_{sph}}{T^3} \quad (5.1)$$

Where $N_f = 3$ is the number of generations. We have to compare now the rate (5.1) with the expansion rate of the Universe given by

$$\chi = \left(\frac{2N^2}{\pi} \right)^{1/2} [(\theta\nu - \nu^2)|\epsilon|]^{1/4} \frac{\mu_{TeV}^2}{M_{Pl}} \quad (5.2)$$

This gives a lower bound on the nucleation temperature provided by

$$\frac{T_n}{\mu_{TeV}} > 3 \times 10^{-12} N [(\theta\nu - \nu^2)|\epsilon|]^{1/4} \quad (5.3)$$

which corresponds to an upper bound on the number of e-folds of inflation as $N_e < 26$. As we have seen in Fig. 5 the nucleation temperature in the available region widely satisfies the bound (5.3).

As we have seen the electroweak phase transition in our model is accompanied by a period of exponential expansion corresponding to a (few) number of e-folds of inflation. After the phase transition the Universe is reheated to a given temperature T_R . If the temperature T_R is higher than the temperature at which $\phi_c(T)/T = 1$ sphalerons will be activated inside the bubbles and the generated baryon asymmetry will be erased. So a third condition is that the reheating temperature be lower than the temperature at which $\phi_c(T)/T = 1$ for a fixed value of the Higgs mass.

In order to understand the temperature at which $\phi_c(T)/T = 1$ for the potential (3.34), we plot for $\mu = \mu_{TeV}$ the value of the ratio $\langle\phi_c(T)\rangle/T$ versus the temperature T (Fig. 6). Here the three lines are calculated for a Higgs of 115 GeV (solid line), 165 GeV (dashed) and 225 GeV (short dashed). In correspondence to these masses the critical temperature T_c^{SM} ¹⁵ has been found, resulting respectively 146, 195 and 250 GeV, at which $\langle\phi_c(T_c)\rangle/T_c$ results approximately 0.2, 0.1 and 0.06¹⁶. A remarkable feature of the SM potential is that, inside a temperature interval of 1 GeV, the origin passes from being a minimum to a maximum and during this change $\langle\phi_c(T)\rangle$ it runs incredibly fast. Clearly this behaviour of $\langle\phi_c(T)\rangle$ remains also at a bit lower temperatures and, in fact, as we can better see in the left panel of Fig. 6, at temperatures of $T \sim 135$, 165 and 190 GeV, respectively, we address $\langle\phi_c(T)\rangle/T \sim 1$.

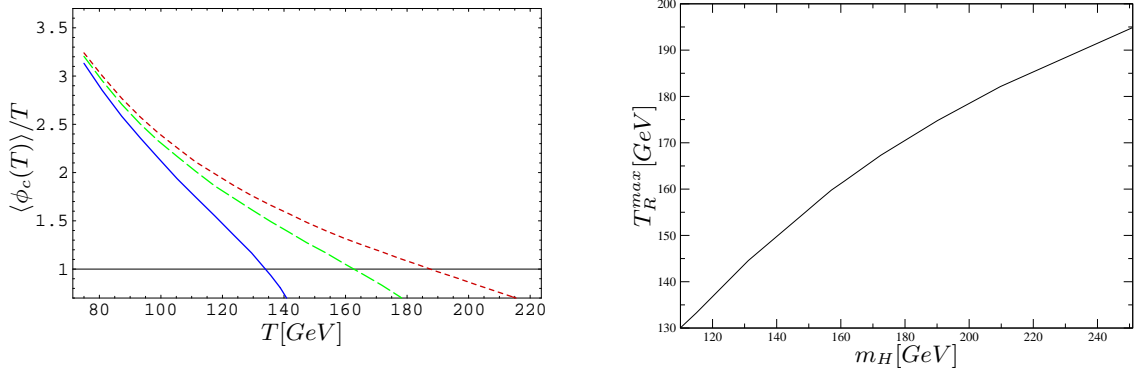


Figure 6: Left panel: Plot of $\langle\phi_c(T)\rangle/T$ as a function of the temperature in GeV for a Higgs mass of 115 GeV (solid line), 165 GeV (dashed) and 225 GeV (short dashed). Right panel: Plot of the temperature at which the SM potential is minimized at $\langle\phi_c(T)\rangle/T = 1$ as a function of the Higgs mass in GeV.

¹⁵Here we define the critical temperature T_c^{SM} as the temperature where the non-trivial minimum of V_{SM} and the origin are degenerate.

¹⁶Of course for such small values of ϕ_c our approximation fails as a consequence of the IR problem of thermal field theories.

We can now compare the maximal reheating temperature as provided by Fig. 6 with the level contours of fixed reheating temperature provided in the various panels of Fig. 4. For a fixed value of the Higgs mass we will first read from the right panel of Fig. 6 the maximal reheating temperature T_R^{max} . Second in the corresponding panel of Fig. 4 we will look for the contour line corresponding to the same value of the reheating temperature for a fixed value of μ_{TeV} . Then the available region in the (θ, ν) plane will be that to the left and below it. For instance if we consider $m_H = 140$ GeV we can see from Fig. 6 that $T_R^{max} \simeq 150$ GeV. Then if we fix $\mu_{TeV} = 1$ TeV and for the $N = 3$ case we see in Fig. 4 that there is a contour line corresponding to $T_R = 0.15 \mu_{TeV} = 150$ GeV and we can easily identify the available region. Now if we increase the Higgs mass we will obtain from Fig. 6 a larger value of T_R^{max} and therefore going back to Fig. 4 the region below and on the left of the corresponding level curve will be bigger than the previous one. For instance if we consider now the Higgs mass $m_H = 180$ GeV we can easily see that $T_R^{max} \simeq 170$ GeV and the corresponding available region will be that below and to the left of the contour line $T_R = 0.17 \mu_{TeV}$, and this region is bigger than the previous one. So for a fixed value of μ_{TeV} the heavier the Higgs boson the bigger the available region in the parameter space.

Another point of view of the same condition is if we instead fix the minimal nucleation temperature, i.e. the maximum number of permitted inflation, in which case the maximal reheating temperature T_R^{max} given by Fig. 6 translates into an upper bound on the value of μ_{TeV} as can be seen in Fig. 7 where the case of $T_n \sim 500$ MeV, equivalent to a number of e-folds $N_e \sim 6$, has been considered.

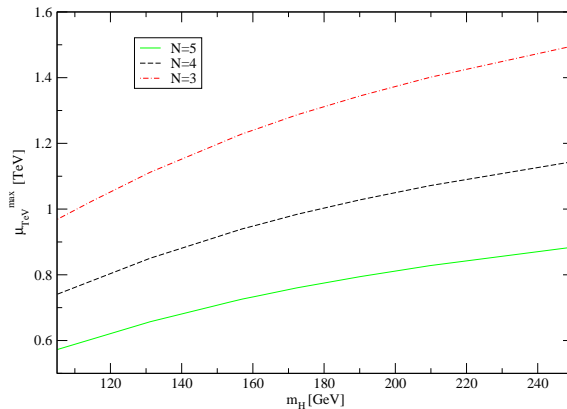


Figure 7: Upper bound on μ_{TeV} for different values of N as a function of the Higgs mass from the condition that $\langle \phi_c(T_R) \rangle / T_R > 1$.

We can conclude that with an additional source of CP-violation¹⁷ the Standard Model

¹⁷This extra source requires by itself extension of the Standard Model. Some mechanisms have been proposed, *e.g.* that in Ref. [43].

with a Higgs boson localized on a brane of a warped space can generate electroweak baryogenesis. A condition for this to happen, as we have seen, is that the universe spans less than 26 e-folds in the supercooling previous to the fast phase transition. This number is close to the number of e-folds required in low-scale inflation to solve the cosmological horizon problem [17]

$$N_e > 30 + \log \frac{T_R}{\mu_{TeV}} . \quad (5.4)$$

In our case condition (5.4) translates into $N_e > 27.7$ which is barely consistent with condition (5.3). We can even stress that in some regions of the available parameter space it might be possible to span the number of e-folds required by Eq. (5.4) although we have not made a dedicated numerical analysis in this paper.

6 Conclusion and Outlook

In this paper we have studied the supercooled electroweak phase transition triggered by the radion in the Randall-Sundrum model at finite temperature in the presence of a Goldberger-Wise potential stabilizing the radion field and deduced the conditions for electroweak baryogenesis coming from the sphaleron interaction rates. We have concentrated in the region of the space of parameters where the theory remains perturbative and the Randall-Sundrum metric is not perturbed by the Goldberger-Wise field. We have estimated from analytical approximations that the contribution of the Higgs field to the Euclidean action is negligible (at least for small Higgs masses) as compared to that of the radion and have worked in the approximation of neglecting the former. Our results can be summarized as follows:

- In the region of the GW parameters consistent with perturbativity there is a wide sub-region where the phase transition is completed provided that the parameter N is not too large. In fact we have found that for $N > 6$ it is very difficult the phase transition to be in agreement with perturbativity constraints.
- In the available region there is always a certain amount of inflation which can go from a few e-folds to larger values. We have explicitly performed our numerical analysis for a moderate maximum value of e-folds ($N_e \leq 6$) although in some tuned regions of the parameter space we might have the number of e-folds required to solve the cosmological horizon problem in low-scale inflationary models ($N_e \sim 30$).
- In parallel with the previous issue we obtain values of the nucleation temperatures much below typical electroweak temperatures¹⁸. This makes sphalerons to decouple inside the bubbles, as required by the condition of not erasing any previously generated baryon asymmetry, independently of the detailed value of the nucleation temperature.

¹⁸As much as we can compare our nucleation temperatures are lower than those obtained in Ref. [15].

- In the analyzed region bubbles percolate and there is no dangerous production of large bubbles that could distort CMB radiation.
- After the phase transition the system reheats to temperatures $T_R/\mu_{TeV} \sim 0.1 - 0.2$. In the presence of supercooling the reheating temperature is essentially insensitive to the precise value of the nucleation temperature.
- At the reheating temperature the condition for the sphaleron to remain decoupled translates into a lower bound on the Higgs mass. Therefore large values of the Higgs mass are favored by electroweak baryogenesis unlike in most models.
- Sphalerons outside the bubbles should be active in order to generate baryon asymmetry in the bubbles wall. The condition for sphalerons to be in thermal equilibrium outside the bubbles translates into an upper bound on the number of e-folds of inflation as $N_e > 26$.
- In the numerical analysis we have considered the case where only the Higgs field is localized on the IR brane. We have checked that similar results hold for the cases where also (part of) the SM fermions are equally localized which would basically translate into a modification of the effective number of light degrees of freedom in the AdS-S phase, as can be seen from Eq. (3.29).

There is a number of open questions and further studies that are worth mentioning here:

- Our numerical analysis has been based on neglecting the Higgs effective potential as compared to the GW radion potential. We believe that this approximation is fully justified for small values of the Higgs mass. However as electroweak baryogenesis in these models seems to favor large over small Higgs masses it should be worthwhile to evaluate the effect of the Higgs potential on the Euclidean action for such heavy Higgses.
- For heavy Higgses the compatibility of the radion and Higgs interactions with electroweak precision tests is an issue and should be considered in detail [44].
- As the CKM phase in the Standard Model is known to be insufficient for a successful electroweak baryogenesis it should be essential to find out some extra source of CP violation in the considered Randall-Sundrum model or extensions thereof.
- As we already mentioned we analyzed numerically cases where the number of e-folds of inflation is moderate, $N_e \leq 6$. However in some regions of our space of parameters we might produce a much stronger inflation and in particular the number of e-folds required to solve the cosmological horizon problem in low-scale inflation. It should be interesting to explore in detail such regions since there the radion might be identified with the inflaton field.

- We have considered a simplified model where the Higgs is fully localized in the IR brane. In other models we could have similar effects. For instance in gauge-Higgs unification models the Higgs field, which arises from the extra-dimensional component of a gauge field, is exponentially localized at the IR brane and the situation seems quite similar to the one we have studied. In Higgsless models the gauge boson masses are provided by the IR boundary conditions and the only sensible way in which the electroweak symmetry could be restored at high temperatures is in the deconfined phase we have described, in which the IR brane disappears. In all of these models the EW phase transition should be similar to that studied in the present paper although dedicated studies should be worthwhile.

Acknowledgments

Work supported in part by the European Commission under the European Union through the Marie Curie Research and Training Networks “Quest for Unification” (MRTN-CT-2004-503369) and “UniverseNet” (MRTN-CT-2006-035863), and in part by CICYT, Spain, under contracts FPA 2004-02012 and FPA 2005-02211.

References

- [1] Lisa Randall and Raman Sundrum. A large mass hierarchy from a small extra dimension. *Phys. Rev. Lett.*, 83:3370–3373, 1999.
- [2] Csaba Csaki, Christophe Grojean, Hitoshi Murayama, Luigi Pilo, and John Terning. Gauge theories on an interval: Unitarity without a higgs. *Phys. Rev.*, D69:055006, 2004.
- [3] Csaba Csaki, Christophe Grojean, Luigi Pilo, and John Terning. Towards a realistic model of higgsless electroweak symmetry breaking. *Phys. Rev. Lett.*, 92:101802, 2004.
- [4] Roberto Contino, Yasunori Nomura, and Alex Pomarol. Higgs as a holographic pseudo-goldstone boson. *Nucl. Phys.*, B671:148–174, 2003.
- [5] Kaustubh Agashe, Roberto Contino, and Alex Pomarol. The minimal composite higgs model. *Nucl. Phys.*, B719:165–187, 2005.
- [6] Kaustubh Agashe and Roberto Contino. The minimal composite higgs model and electroweak precision tests. *Nucl. Phys.*, B742:59–85, 2006.
- [7] Roberto Contino, Leandro Da Rold, and Alex Pomarol. Light custodians in natural composite higgs models. 2006.
- [8] M. Quiros. Field theory at finite temperature and phase transitions. *Helv. Phys. Acta*, 67:451–583, 1994.

- [9] V. A. Rubakov and M. E. Shaposhnikov. Electroweak baryon number non-conservation in the early universe and in high-energy collisions. *Usp. Fiz. Nauk*, 166:493–537, 1996.
- [10] Marcela Carena and C. E. M. Wagner. Electroweak baryogenesis and higgs physics. 1997.
- [11] Antonio Riotto and Mark Trodden. Recent progress in baryogenesis. *Ann. Rev. Nucl. Part. Sci.*, 49:35–75, 1999.
- [12] Marcela Carena, M. Quiros, and C. E. M. Wagner. Electroweak baryogenesis and higgs and stop searches at lep and the tevatron. *Nucl. Phys.*, B524:3–22, 1998.
- [13] Paolo Creminelli, Alberto Nicolis, and Riccardo Rattazzi. Holography and the electroweak phase transition. *JHEP*, 03:051, 2002.
- [14] Walter D. Goldberger and Mark B. Wise. Phenomenology of a stabilized modulus. *Phys. Lett.*, B475:275–279, 2000.
- [15] Lisa Randall and Geraldine Servant. Gravitational waves from warped spacetime. 2006.
- [16] Jared Kaplan, Philip C. Schuster, and Natalia Toro. Avoiding an empty universe in rs i models and large-n gauge theories. 2006.
- [17] Lloyd Knox and Michael S. Turner. Inflation at the electroweak scale. *Phys. Rev. Lett.*, 70:371–374, 1993.
- [18] Juan M. Maldacena. The large n limit of superconformal field theories and supergravity. *Adv. Theor. Math. Phys.*, 2:231–252, 1998.
- [19] Edward Witten. Anti-de sitter space and holography. *Adv. Theor. Math. Phys.*, 2:253–291, 1998.
- [20] Nima Arkani-Hamed, Massimo Porrati, and Lisa Randall. Holography and phenomenology. *JHEP*, 08:017, 2001.
- [21] R. Rattazzi and A. Zaffaroni. Comments on the holographic picture of the randall-sundrum model. *JHEP*, 04:021, 2001.
- [22] Steven S. Gubser. Ads/cft and gravity. *Phys. Rev.*, D63:084017, 2001.
- [23] Per Kraus. Dynamics of anti-de sitter domain walls. *JHEP*, 12:011, 1999.
- [24] Edward Witten. Anti-de sitter space, thermal phase transition, and confinement in gauge theories. *Adv. Theor. Math. Phys.*, 2:505–532, 1998.

- [25] Walter D. Goldberger and Mark B. Wise. Modulus stabilization with bulk fields. *Phys. Rev. Lett.*, 83:4922–4925, 1999.
- [26] O. DeWolfe, D. Z. Freedman, S. S. Gubser, and A. Karch. Modeling the fifth dimension with scalars and gravity. *Phys. Rev.*, D62:046008, 2000.
- [27] Csaba Csaki, Michael Graesser, Lisa Randall, and John Terning. Cosmology of brane models with radion stabilization. *Phys. Rev.*, D62:045015, 2000.
- [28] L. Dolan and R. Jackiw. Symmetry behavior at finite temperature. *Phys. Rev.*, D9:3320–3341, 1974.
- [29] Steven Weinberg. Gauge and global symmetries at high temperature. *Phys. Rev.*, D9:3357–3378, 1974.
- [30] D. A. Kirzhnits and Andrei D. Linde. Macroscopic consequences of the weinberg model. *Phys. Lett.*, B42:471–474, 1972.
- [31] D. A. Kirzhnits and Andrei D. Linde. A relativistic phase transition. *Sov. Phys. JETP.*, 40:628, 1975.
- [32] D. A. Kirzhnits and Andrei D. Linde. Symmetry behavior in gauge theories. *Ann. Phys.*, 101:195–238, 1976.
- [33] Paul Fendley. The effective potential and the coupling constant at high temperature. *Phys. Lett.*, B196:175, 1987.
- [34] David J. Gross, Robert D. Pisarski, and Laurence G. Yaffe. Qcd and instantons at finite temperature. *Rev. Mod. Phys.*, 53:43, 1981.
- [35] M. E. Carrington. Ring diagram summations in the finite temperature effective potential. *Can. J. Phys.*, 71:227–236, 1993.
- [36] Alan H. Guth and S. H. H. Tye. Phase transitions and magnetic monopole production in the very early universe. *Phys. Rev. Lett.*, 44:631, 1980.
- [37] Alan H. Guth and Erick J. Weinberg. Could the universe have recovered from a slow first order phase transition? *Nucl. Phys.*, B212:321, 1983.
- [38] Michael S. Turner, Erick J. Weinberg, and Lawrence M. Widrow. Bubble nucleation in first order inflation and other cosmological phase transitions. *Phys. Rev.*, D46:2384–2403, 1992.
- [39] Andrei D. Linde. Decay of the false vacuum at finite temperature. *Nucl. Phys.*, B216:421, 1983.
- [40] Peter Arnold and Larry D. McLerran. Sphalerons, small fluctuations and baryon number violation in electroweak theory. *Phys. Rev.*, D36:581, 1987.

- [41] Jan Ambjorn, M. L. Laursen, and M. E. Shaposhnikov. Baryon asymmetry generation in the electroweak theory: A lattice study. *Nucl. Phys.*, B316:483, 1989.
- [42] M. E. Shaposhnikov. Baryon asymmetry of the universe in standard electroweak theory. *Nucl. Phys.*, B287:757–775, 1987.
- [43] Micha Berkooz, Yosef Nir, and Tomer Volansky. Baryogenesis from the kobayashi-maskawa phase. *Phys. Rev. Lett.*, 93:051301, 2004.
- [44] John F. Gunion, Manuel Toharia, and James D. Wells. Precision electroweak data and the mixed radion-higgs sector of warped extra dimensions. *Phys. Lett.*, B585:295–306, 2004.